Preprints (www.preprints.org) | NOT PEER-REVIEWED | Posted: 14 December 2017 doi:10.20944/preprints201712.0094.v1

Peer-reviewed version available at Energies 2018, 11, 447; doi:10.3390/en11020447

# Prediction Model of Photovoltaic Module Temperature for Power Performance of Floating PVs

Waithiru Charles Lawrence K.[1], Jong Rok Lim[1], Chang Sub Won[2], and Hyungkeun Ahn [1]

[1]Konkuk University, 120 Neungdong-ro, Gwanjin-gu, Seoul 143-701, Korea

[2]LSIS R&D Campus 116 beongil 40 Anyang, Gyeonggi 431831, Korea

**Abstract: Rapid reduction in the $/Wp prices of photovoltaic (solar PV) energy has been proceeded recently, resulting in near exponential deployments with an annual capacity of 200 GW expected by 2020. Achieving high efficiency is necessary for many solar manufacturers to break even. In addition, new innovative installation methods are emerging to complement the improvement of system performance. The floating PV (FPV) solar market space has emerged over the past decade as a method for utilizing the cool ambient environment of the FPV system near the water surface to boost the power output performance of the PV module and ultimately the yield of the PV system. PV module temperature, which is the most critical factor affecting efficiency, ultimately governs the effective performance of solar cells, module, and all semiconductor materials in general. We propose the first ever electrical efficiency equations ($\eta_{c,FPV_1}$ and $\eta_{c,FPV_2}$) for an FPV module installed on water based on two new predictions of FPV temperature operation models ($T_{m_1}$ and $T_{m_2}$), whose coefficients are derived from FPV site data with MATLAB. The theoretical prediction of module temperature shows respective errors of 2% and 4% when compared to the FPVM measured data.**

**Index terms: Floating PV Systems (FPV); Floating PV Module (FPVM)**

## I. INTRODUCTION

A report published by IRENA in 2016 [1] shows that the global cumulative capacity of installed solar systems was 222 GW, with China, Germany, Japan, and USA installing 43 GW, 40 GW, 33 GW and 22 GW, respectively. In many markets, we see the growing conflict between environmentalists and solar enthusiast concerning installation land policy. A new and innovative installation method to cater to the installations of the future is necessary. A floating photovoltaic (PV) system is one such method that utilizes the cooling effect of water on its surface to improve the efficiency of the PV module and ultimately the performance of the PV system, with minimal interference with the marine environment.

Extensive studies on the efficiency, power, and temperature of the conventional PV system module have been carried out by Evans and Florschutez [2], Duffie and Beckman [3], and many others [4]. Considering the importance of device temperature in efficiency analysis, model 1 proposed in this paper correlates the temperature of the FPV module (FPVM) to the ambient temperature, solar radiation, and wind speed of the FPV environment. The influence of water temperature of the FPV installation is incorporated in model 2. When compared to the field data of a real FPVM, the average error of models 1 and 2 is 2% and 4%, respectively. The two temperature models are based on analysis of data obtained for 5 min from two FPV sites on Hapcheon lake in Korea. Important comparisons are performed with ten reference temperature models and the resulting findings are presented. The characteristic analysis of the FPV models shows resemblance to that of the models proposed by Lasnier and Ang 1990 [5] and Duffie and Beckmans 2006 [3]. Duffie and Beckmans predictions are thus preferred for size optimization, simulation and design of solar photovoltaics. Kurtz [6], Koehl [7] and Skoplaski[8] that include wind speed in temperature predictions are also included in analysis. A simple comparison of the temperature profiles of FPVMs with the conventional land- or rooftop-based modules shows that the mean value of the yearly PV module temperature of an FPV system is 21 °C, which is 4 °C below that of conventional PV modules, translating into 10% more kWh energy production by the FPV system.

The aforementioned research is important in analyzing the correlation between efficiency and temperature. Solar cells only convert a small amount of absorbed solar radiation into electrical energy with the remaining energy being dissipated as heat in the bulk region of the cell [9],[10]. A rise in the operation temperature of a solar cell and module reduces the band gap, thus slightly increasing the short circuit current of a solar cell for a given irradiance, but largely decreasing the open circuit voltage, resulting in lower fill factor and power output. The net effect results in a linear relation for the electrical efficiency ($\eta_c$) of a PV

Corresponding Author Telephone: +821046309972

Email: hkahn@konkuk.ac.kr

*Preprints* (www.preprints.org) | NOT PEER-REVIEWED | Posted: 14 December 2017 doi:10.20944/preprints201712.0094.v1

Peer-reviewed version available at *Energies* **2018**, *11*, 447; doi:10.3390/en11020447

module as follows:

$$\eta_c = \eta_{Tref}\left[1 - \beta_{ref}\left(T_m - T_{ref}\right)\right] \quad (1)$$

where $\eta_{Tref}$ and $\beta_{ref}$ are the electrical efficiency and temperature coefficient of the PV module, respectively, with the values of 14.5% and 0.004 $K^{-1}$, respectively, for the FPV analysis case.. $T_m$ and $T_{ref}$ is the PV module operational temperature and reference temperature respectively.

Based on the two predictions of the temperature of an FPVM proposed herein, we propose two corresponding modifications to Equation (1) based on the input parameters of $T_m$ as follows:

$$\eta_{c,FPV_1} = \eta_{Tref}[1 - \beta_{ref}(2.0458 + 0.9458T_a + 0.0215G_T - 1.2376V_w - T_{ref})] \quad (2)$$

$$\eta_{c,FPV_2} = \eta_{Tref}[1 - \beta_{ref}(1.8081 + 0.9282T_a + 0.021G_T - 1.2210V_w + 0.0246T_w - T_{ref})] \quad (3)$$

where $\eta_{c,FPV}$, $T_a$, $G_T$, and $V_w$ represent average values of efficiency, ambient temperature, solar irradiation, and wind speed of the FPVM. Equation (3) includes an additional variable, i.e., water temperature ($T_w$).

As discussed later, Equation (2) is shown as a graphical illustration in Fig. 7 demonstrating a reduction in the efficiency of FPVM by 0.058% per 1 °C increase in the temperature of the FPVM.

## II. FLOATING PV SYSTEM

### *A. Site Information of Floating PV System*

Fig. 1 shows the aerial views of Korea's first 100 kW and 500 kW Hapcheon Dam FPV power stations located at southern part of the country. Commercial 1MW rooftop PV station 36 mi far from FPVs is selected for the comparison also in Table 1. Based on the previous research on module reliability [14], a special anti-damp proof FPVM with a unique encapsulation [9] was certified and installed. A unique mooring system designed locally anchored the floating system on the dam floor, aligning the FPV system to the correct azimuth. A weather station was installed on the floating platform with radiation sensors, temperature sensors to monitor water temperature and the temperature of the FPV module, GPS positioning sensors, an anemometer to monitor wind speed, and a security camera for a visual view under severe weather situation such as typhoons. Data acquisition was based on IEC standard 61724[10].A low-loss cable transmitted DC power from the FPV system to dry land where an electric room housing a PV inverter and monitoring computers were installed.


Fig. 1. Aerial view of the 100 kW (left) and 500 kW (right) floating systems on Hapcheon lake

Table 1. FPVs and Rooftop PVs information

| Project Type | Test bed | Commercial | |
|---|---|---|---|
| | | Floating PV | *Rooftop PV |
| Site Name | Hapcheon Dam 100kW | Hapcheon Dam 500kW | Haman 1MW |
| Site coordinates | N 35.5º 33'36" | E 128º 02' 26" | N 35.5º 33'36" |
| Installation Capacity | 100kW | 500kW | 1MW |
| Installation Date | 2011 Nov. | 2012 June | 2012 |
| Module Slope | 33º | 33º | 30º |
| Module type | c-Silicon | c-Silicon | c-Silicon |
| Module# | 417pcs | 1,667pcs | 4,000pcs |
| Mounting | Aluminum, Steel | Aluminum | Aluminum |
| Mounting type | Fixed | Fixed | Fixed |
| Water Depth /*Location | 20 meters | 40 meters | *36 mi from FPVs |

### *B. Power Outputs of Floating PV versus Rooftop-based System*

In Table 2, we compare the floating systems of capacities 100 kW and 500 kW with a rooftop system of capacity 1,000 kW, located 60km southeast of the 100kW site. The output summary is given in Table 2

Table 2. General system performance and output

| Project Type | | Floating PV | | Rooftop PV |
|---|---|---|---|---|
| | | 100kW | 500kW | 1MW |
| Annual Output (kWh/year) Avg. | | 130,305 | 693,219 | 1,197,547 |
| Monthly Output (kWh/year) Avg. | | 357 | 1,859 | 3,281 |
| Normalized Power | kWh/KWp/year | 1,303 | 1,386 | 1,198 |
| | kWh/KWp/day | 3.58 | 3.80 | 3.28 |

Corresponding Author Telephone: +821046309972
Email: hkahn@konkuk.ac.kr

*Preprints* (www.preprints.org) | NOT PEER-REVIEWED | Posted: 14 December 2017 doi:10.20944/preprints201712.0094.v1

Peer-reviewed version available at *Energies* **2018**, *11*, 447; doi:10.3390/en11020447

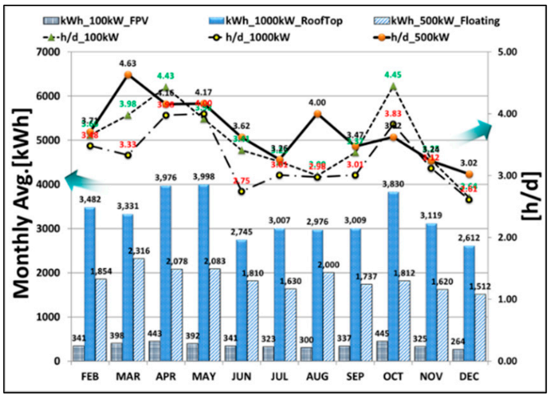


Fig. 2. Average Monthly Power (kWh) output comparison for 2012 of 100 kW, 500 kW floating systems (Hapcheon dam) ; and 1000 kW rooftop system at Haman site (2013).

Table 2 shows yearly energy results of the three PV stations. As shown in Table 2, the y-axis (left) is the monthly average energy output. For example in April 2013, average monthly output from the three PV Systems was 443kWh, 2078kWh and 3976kWh for the 100kW, 500kW and 1000kWPV systems respectively. Multiplying respective monthly average but days in month, and summing monthly outputs gives 130.3MWh, 693.2MWh and 1,197.5MWh respective total yearly output.

For the 100kW FPV station, October and December are the best and worst performing month at 445kWh and 264kWh respectively, compared to the station's yearly average of 357kWh. Similarly for the 500kW FPV station, March and December are the best and worst performing month at 2,316kWh and 1,512kWh respectively, compared to the station's yearly average of 1,859kWh. Finally for the 1,000kW rooftop PV station, May and December are the best and worst performing month at 3,998Wh and 2,612kWh respectively, compared to the station's yearly average of 3,281kWh. Whereas the rooftop produces more power quantitatively, the FPV systems are more efficient in qualitative power delivery.

With reference to y-axis on the right, output energy is normalization to name plate peak power (kWp) with units hours per day (h/d). Table 2 shows an average of monthly values giving yearly normalized output as 3.58 h/d, 3.80 h/d, and 3.28 h/d, for the 100kW, 500kW and 1000kW sites respectively, as shown in Table 2. Analysis of the latter values proves the two FPV systems are outperforming the rooftop systems by 9% and 16%, warranting investigation into temperature performance.

## III. FLOATING PV TEMPERATURE MODEL

In this section, we formulate a multiple linear equation for the dependent variable ($y$; FPV module operation temperature) using four independent linear variables $x_1, x_2, x_3$, and $x_4$ representing solar irradiance ( $G_T$ ), ambient temperature ($T_a$), wind speed ($V_w$), and water temperature ($T_w$), respectively.

Table 3. Multiple regression variables for FPVM temperature (symbol; Tm)

| Term | Predictor Variables | Symbol | Unit |
|---|---|---|---|
| $x_1$ | Ambient temp. | $T_a$ | °C |
| $x_2$ | Irradiance | $G_T$ | W/m² |
| $x_3$ | Wind Speed | $V_w$ | m/s |
| $x_4$ | Water temp. | Tw | °C |

The multiple linear equation is linear for unknown parameters$\beta_0 - \beta_{k-1}$, and is of the form given in Equation (4).

$$y_i = \beta_0 + \beta_1 x_{i1} + \beta_2 x_{i2} + \cdots + \beta_{k-1} x_{ik-1} + \epsilon_i (4)$$

for $i = 1(1)n$, where $y_i$ is the predicted value of y, and assumes $i^{th}$ independent error $\epsilon_i \sim N(0, \sigma^2)$ following a normal distribution with independent mean and variance squared. The matrix can be expressed as

$$Y = X\beta + \epsilon \qquad (5)$$

where

$$Y = \begin{pmatrix} Y_1 \\ Y_2 \\ \vdots \\ Y_n \end{pmatrix}, \ \beta = \begin{pmatrix} \beta_1 \\ \beta_2 \\ \vdots \\ \beta_n \end{pmatrix}, \ \epsilon = \begin{pmatrix} \epsilon_1 \\ \epsilon_2 \\ \vdots \\ \epsilon_n \end{pmatrix} \ \text{and}$$

$$X = \begin{pmatrix} 1 & x_{11} & x_{12} & \cdots & x_{1k-1} \\ 1 & x_{21} & x_{22} & \cdots & x_{2k-1} \\ \vdots & \vdots & \vdots & \cdots & \vdots \\ 1 & x_{n1} & x_{n2} & \cdots & x_{nk-1} \end{pmatrix}.$$

The multiple linear regression form is expressed in equation (5) with Y, β, ϵ, and X representing $y$ observations, vector of parameters, error, and $n \times k$ matrix vectors, respectively. The goal is to estimate the model parameters.

The field data of floating PV are given in the forms of $Y_i, x_{i1}, x_{i2}, x_{i3}$, and $x_{i4}$, for $T_m, T_a, G_T, V_w$, and $T_w$, respectively.

We use the standard least-squares minimization to determine the aforementioned model parameters by minimizing the sum of squares of residuals ($SS_{Res}$) as shown in a matrix form in equation (6).

$$SS_{Res} = \sum_1^n e_i^2 \qquad (6)$$

where $e = (Y - \hat{Y})$ and $\hat{Y} = \hat{\beta}_0 + \hat{\beta}_1 x_1 + \hat{\beta}_2 x_2 + \cdots + \hat{\beta}_{k-1} x_{k-1}$.

Corresponding Author Telephone: +821046309972
Email: hkahn@konkuk.ac.kr

Preprints (www.preprints.org) | NOT PEER-REVIEWED | Posted: 14 December 2017 doi:10.20944/preprints201712.0094.v1

Peer-reviewed version available at Energies 2018, 11, 447; doi:10.3390/en11020447

Substituting the former into Equation (6) leads to the definition of $SS_{Res}$ in terms of the unknown parameters in equation (7).

$$SS_{Res} = \sum_1^n (Y-\hat{Y})^2 = (Y-\hat{Y})'(Y-\hat{Y}) = Y'Y - 2\hat{\beta}'X'Y' + \hat{\beta}'X'X'\hat{\beta} \quad (7)$$

where equation is expanded using $\hat{Y} = X\hat{\beta}$. Integrating $SS_{Res}$ with respect to $\hat{\beta}$ results in normal equations, which have to be solved for unknown equations in Equation (8). For easy computation, an alternative matrix equation is presented for solving the coefficients.

$$\frac{\partial SS_{Res}}{\partial \hat{\beta}} = \frac{\partial (Y'Y - 2\hat{\beta}'X'Y' + \hat{\beta}'X'X'\hat{\beta})}{\partial \hat{\beta}} \quad (8)$$

$$\hat{\beta} = (X'X)^{-1} + X'Y \quad (9)$$

where $X'$ is the inverse $X$ matrix of predictor variables listed on Table 3

Our X matrix contains more than 100,000 data points, as is plotted in Fig.3, and corresponds to FPV data collected every 5 min in 2013. The Y matrix corresponds to the measured module temperature. The coefficients of models 1 and models 2 in Equation4 for the FPVM suggested in this paper are expressed as follows.

$$T_{m_1} = 2.0458 + 0.9458T_a + 0.0215G_T - 1.2376V \quad (10)$$

$$T_{m_2} = 1.8081 + 0.9282T_a + 0.021G_T - 1.2210V_w + 0.0246T_w \quad (11)$$

$T_{m_1}$ and $T_{m_2}$ explains the operation temperature behavior of the FPVM with seasonal variables $T_a$, $G_T$, $V_w$ and $T_w$.

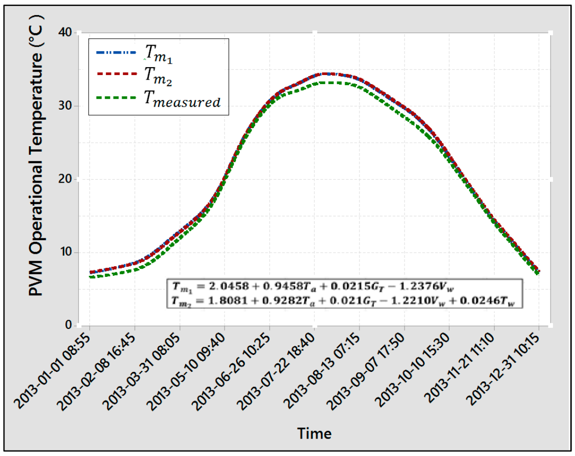


Fig.3 2013 PV module temperature data; measured and modeled data (100 kW PV system)

Fig.3 below, is a time series plot of $T_{m_1}$, $T_{m_2}$ and $T_{measured}$ for 2013. $T_{measured}$ is actual FPV measured data. From the graph, predicted PVM temperatures are almost always higher than measured except during second quarter (Q2) where $T_{measured} > T_{m_1}$, $T_{m_2}$. Coincidentally, wind speeds ($T_W$) are also low during same period, implying the dominance of $T_W$ in the two models Equation 10 and Equation11.

Equation12 introduces the average error of FPV models, by comparing real to predicted values as shown. Calculations show $T_{Error}$ ranging 2.06% and 4.40%, for respective FPV models;

$$T_{Error} = \int_{n=1}^{n=k} (T_{measured} - T_m) \quad (12)$$

where $k$ are total data points. Inclusion of $T_w$ in Equation11 increases the error by 2% when compared to Equation10.

## IV. FPV MODEL COMPARISON

### A. Comparison with Land-based PV System

In this section, we compare the FPV with 1 MW rooftop system whose information is given in Table 1. It is evident the FPV system produces a large portion of energy at lower temperatures [14].

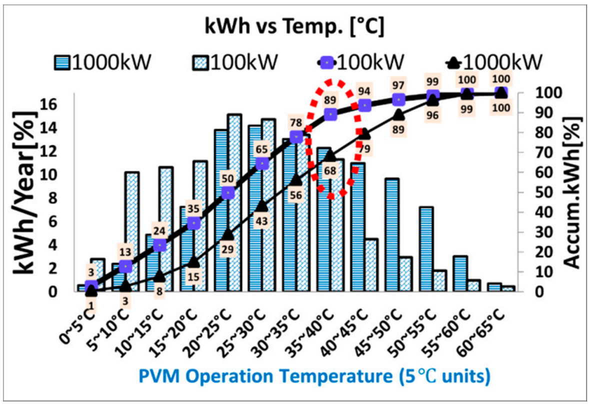


Fig 4. Energy output (kWh) of floating PV verses rooftop PV for various module temperatures.

Fig4 illustrates the correlation between PV power output (kWh) and corresponding module temperature when respective power is produced. 100% of energy produced by the 100kW site is 130MWh, while energy produced by the 1000kW site is 1,197MWh per year. This two MWh outputs occur when PVM operation temperature varies periodically between the lowest (0°C) and the highest value (65°C). Using Minitab statistical software, yearly energy is sorted based on corresponding module temperature, as shown in Fig.4. For example, with reference to the 20~25°C range, 15% of 130MWh and 14% of 1,197MWh is

Corresponding Author Telephone: +821046309972
Email: hkahn@konkuk.ac.kr

Preprints (www.preprints.org) | NOT PEER-REVIEWED | Posted: 14 December 2017 doi:10.20944/preprints201712.0094.v1

Peer-reviewed version available at *Energies* **2018**, *11*, 447; doi:10.3390/en11020447

produced by the two respective PV sites.

With reference to y-axis (right) on the Fig.4, cumulative energy for respective temperature ranging from 0°C to 65°C is plotted against corresponding energy (kWh) increasing from 0% to 100% of total yearly output. Cumulatively, 89% of all energy produced by the FPV system, and 68% of all energy delivered by the rooftop system occurs when module temperatures of both systems are below 40°C, as indicated. Energy produced beyond the 25°C Standard Test Condition (STC) condition has the negative power loss effect due to loss of open circuit ($V_{oc}$) and fill factor (F.F.) [9]. As is evident, a larger percentage of cumulative energy of the FPV is produced at lower temperatures.

*B. Comparison with Selected Temperature Models*

A select group of PV temperature models [4] is presented in Table 4 for comparison. The models incorporate a reference state for example air temperature ($T_a$), and the corresponding values of relevant variables ($G_T$, $V_w$, etc.). Owing to the complexities involved, some authors presented explicit correlation in addition to implicit relations requiring iterations.

Table 4. PV module models

| Model | Empirical Models |
|---|---|
| Ross (1976)[15] | $T_c = T_a + kG_T \quad where\ k = \Delta(T_c - T_a)/\Delta G_T$ |
| Rauschenbach (1980)[16] | $T_c = T_a + (G_T/G_{T,NOCT})(T_{c,NOCT} - T_{c,NOCT})(1 - \frac{n_m}{\gamma_\alpha})$ |
| Risser & Fuentes(1983)[19] | $T_c = 3.81 + 0.0282 \times G_T 1.31 \times T_a - 165V_w$ |
| Schott (1985)[20] | $T_c = T_a + 0.028 \times G_T - 1$ |
| Ross & Smokler (1986) [16] | $T_c = T_a + 0.035 \times G_T$ |
| Mondol et al., ('05,'07) | $T_c = T_a + 0.031G_T$<br>$T_c = T_a + 0.031G_T - 0.058$ |
| Lasnier & Ang (1990) [5] | $T_c = 30.006 + 0.0175(G_T - 300) + 1.14(T_a - 25)$ |
| Servant (1985)[21] | $T_c = T_a + \alpha G_T(1 + \beta T a)(1 - \gamma V_w)(1 - 1.053 n_{m,ref})$ |
| Duffie & Beckman [3] | $T_c = T_a + (G_T/G_{NOCT})(9.5/5.7 \times 3.8V_w)(T_{NOCT} - T_{a,NOCT})(1 - n_m)$ |
| Koehl (2011) [7] | $T_c = T_a + G_T/(U_0 + U_1 \cdot V_w)$ |
| Kurtz S (2009) [6] | $T_c = T_a + G_T \cdot e^{-3.473 - 0.0594 \cdot V_w}$ |
| Skoplaki (2008) [8] | $T_c = T_a + (G_T/G_{NOCT}) \cdot (T_{NOCT} - T_{a,NOCT}) \cdot h_{w,NOCT}/h_w \cdot [1 - \eta_{STC}/\tau \cdot \alpha\,(-\beta_{STC} T_{STC})]$ |

In Fig.5 below, models listed in Table 4 above are plotted against both ambient ($T_a$) temperature, and solar radiation ($G_T$).

.

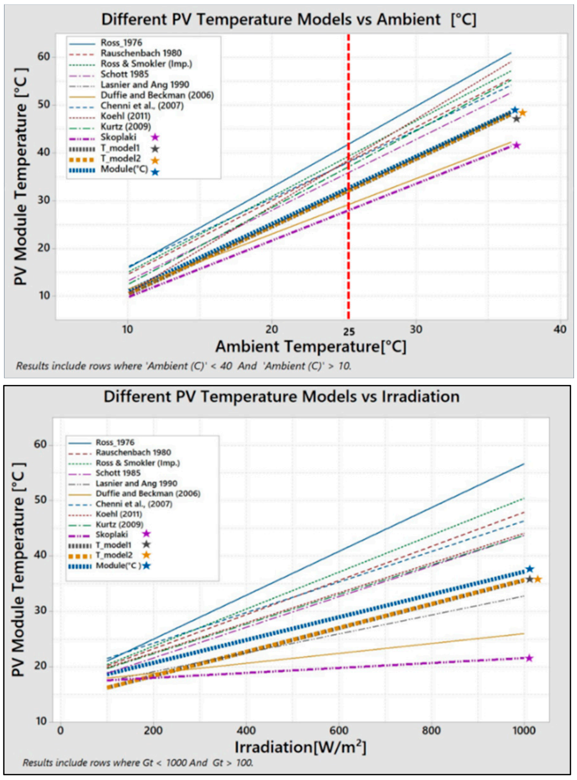


Fig 5. PV predicted cell/module temperature verses ambient temperature (Top) and irradiance (Bottom)

As can be seen, all models vary linearly with both $T_a$ and $G_T$ with varying model specific gradients. The implication is difference model interpret heat dissipation by the PV module differently when exposed to the elements. For example, Ross [16] and Rauschenbach [17] model display the highest PV operation temperatures when exposed to $G_T$ at constant $T_a$. Koehl, Kurtz and Skoplaki's research incorporates wind ($V_w$) data in temperature prediction.

In Fig.5 (top), Duffie & Beckman and Skoplaki [8] record low temperatures with increasing $T_a$ suggesting adequate heat dissipation by the modules due to incorporation of wind data. To the contrary, Ross and Rauschenbach show high temperatures near 60°C suggesting the PVM retains heat. Model 1 ($T_{m1}$) and Model2 ($T_{m2}$) plots are almost identical, and vary slightly with real PV module data, and operate at much lower temperatures than all other models.

In Fig.5 (bottom), Skoplaki has lowest operation temperature with increasing $G_T$, while Ross has highest temperature values because of PVM heat retention. Skoplaki model reacts very slowly to rising $G_T$ due to quick heat dissipation by the $V_w$ factor. A slight deviation from real

Corresponding Author Telephone: +821046309972
Email: hkahn@konkuk.ac.kr

Preprints (www.preprints.org) | NOT PEER-REVIEWED | Posted: 14 December 2017 doi:10.20944/preprints201712.0094.v1

Peer-reviewed version available at Energies 2018, 11, 447; doi:10.3390/en11020447

temperature by Model 1 ($T_{m1}$) and Model2 ($T_{m2}$) is noted with increasing $G_T$ .

Based on the two graphs in Fig.5, we conclude that our two FPV models operating temperatures are significantly lower than conventional PV module ranges.

*C. Comparison of Models with Minitab Model*

Minitab has well-defined algorithms that describe the change of any dependent variable $y$ with the interaction between the respective independent variables $x_i$ . Refer to Appendix 1 for graphs showing the interaction between independent variables. Minitab generates an equation that shows the interaction between the dependent variable (module temperature) and independent variables. The Minitab equation (12) shown below is highly accurate (0.1%) but incurs the risk of equation complexity due to over-fitting.

Module =
$-1.9034 + 1.12322\, x_1 + 0.028655\, x_2 - 0.6517\, x_3$
$- 0.09362\, x_4 - 0.001328\, x_1^2$
$- 0.000014\, x_2^2 + 0.08382\, x_3^2$
$- 0.000604\, x_1 \cdot x_2 - 0.031334\, x_1 \cdot x_3$
$+ 0.001389\, x_1 \cdot x_4 - 0.000981\, x_2 \cdot x_3$
$+ 0.000545\, x_2 \cdot x_4 + 0.039145\, x_3 \cdot x_4$

for $x_1, x_2, x_3, x_4$, representing $T_a, G_T, V_w, T_w$.

In Fig.6, four histograms compare the normal distribution of real FPV module temperature data to Model 1, Model 2, Minitab's predicted values.

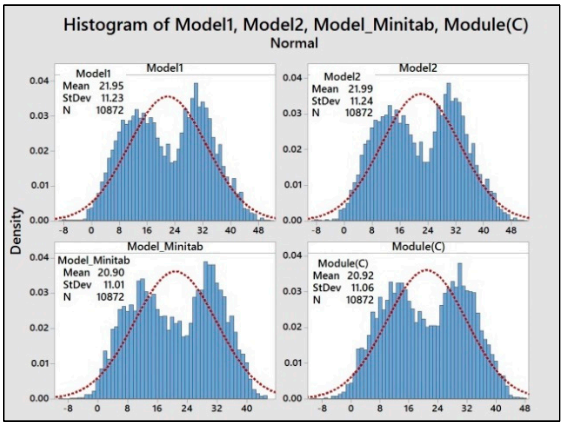


Fig 6. Comparison of all three FPV models (left); Histograms of temperature predictions; Minitab, model 1, model 2, and actual temperature (right)

The x-axis shows operational temperature from -10°C to over 50°C. Y-axis plots the density of respective temperature range throughout the year. All model distributions show a bimodal shape, with 2 peaks temperatures at 10°C and 30°C. The dotted red line shows the normal distribution curve of respective data.

Mean values are 21.95°C, 21.99°C, 20.90°C and 20.92°C for Model 1, Model 2, Minitab's and to real field data (Module(C)). When compared to real data, mean errors as 4.92%, 5.11%, 0.1% and 0.0% (base value) for the respectively values. A 0.1% error is indicative of the Minitab model's high accuracy in comparison to real measured data. The behavior of a plot of Equation12 is identical to $T_{measured}$ in Fig.3.

## V. FPV MODEL EFFICIENCY AND POWER PREDICTION

Operating a PV system on the water surface has the added benefit of increasing conversion efficiency due to the cooling effect on water's surface.

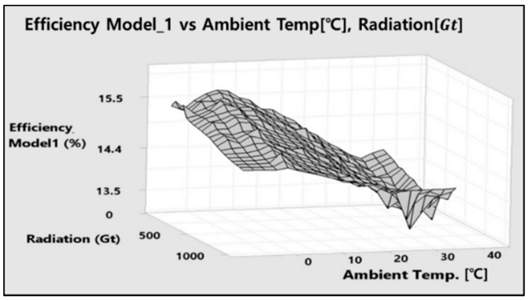


Fig 7. 3D surface plots of Model 1 efficiency/Ta/Gt

Fig. 7 is a 3D plot of FPV module efficiency/ $T_a$ / $G_T$ . In the plot, a decrease in ambient temperature ($T_a$) has a positive effect of increasing efficiency between 1% ~ 2% points. The plot shows the importance $T_a$ in defining PVM operation temperature and ultimately conversion efficiency. Radiation ($G_T$) plays a secondary role given the minimal impact on efficiency. It can be observed that, at higher radiation level $G_T$ is varying more frequently, and this impacts power stability.

In summary, as observed from the FPV data, low ambient conditions are ideal for higher system efficiency and power performance as shown by seasonal variation in efficiency in Fig 8. In June through August when ambient temperature are high, PVM efficiency drops between 1~2% points. For a land based system, a more severe dip is expected. During fall and winter when temperature drop, we notice a step rise in efficiencies to mid-15% level. Based on graphical description on Fig.8, for FPV module temperature models 1, we predict that a 1 ℃ increase in $T_m$ results in a 0.058% decrease in $\eta_{c,FPV_1}$ , as shown for in Equation13 .

Corresponding Author Telephone: +821046309972
Email: hkahn@konkuk.ac.kr

*Preprints* (www.preprints.org) | NOT PEER-REVIEWED | Posted: 14 December 2017 doi:10.20944/preprints201712.0094.v1

Peer-reviewed version available at *Energies* **2018**, *11*, 447; doi:10.3390/en11020447

$$\eta_{c,FPV_1} = 15.96 - 0.058T_{m_1} \quad (13)$$

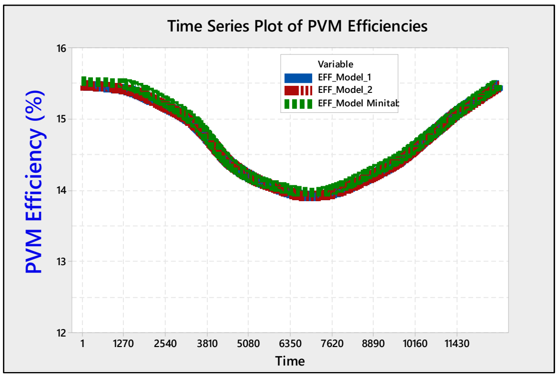


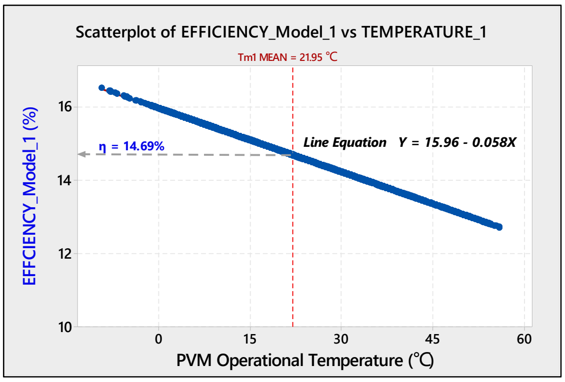


Fig.8 FPV efficiency/Model FPV(Tm) and FPV (100kW) versus efficiency Gt.

Operational temperature has an important role in the energy conversion process [22]. From Fig 8, the electrical efficiency of the PV module depends linearly on the operation temperature as shown. Latifa's [23] has done important work (2014) comparing crystalline (c-Si) and amorphous silicon (a-Si) coefficients per °C. This work shows coefficient values for a-Si closely identical to FPV.

## VI. CONCLUSION

A floating PV system was installed in 2011, and its floating module temperature is analyzed in this paper. The theoretical prediction of module temperature shows an error in the range of 2%–4% when compared to the measured data. The performance ratios (PR) on both the AC and DC sides were analyzed, which showed that the floating PV system exhibits PR 10% better than that of a land-based system. The results suggest lower thermal losses associated with thermal heating of the FPV modules owing to cool temperature environment near the water surface. The analysis of the FPV module operation model showed the critical role played by low ambient conditions in boosting the operation efficiency of the PV system module.

Two prediction models of the FPV module temperature are suggested for the analysis of performance of the FPV module and system. Model 1 includes the effects the independent variables, i.e., ambient temperature (Ta), solar irradiance (Gt), and wind speeds (Vw). When compared to the measured data, the equation error of model 1 is 2%. Model 2 includes the three aforementioned independent variables in addition to water temperature (Tw). Although the error of model 2 increases slightly to 4%, the results are within the reasonable range of error.

Through this research, a correlation between the temperature of the operating environment and system efficiency is derived. Beyond solar irradiation of 100 W/m², the floating system records an ideal efficiency averaging more than 14.69% based on yearly mean PVM temperature of 21.95°C. It was observed that approximately two-thirds (68%) of the annual yield was produced by the FPV system when the module temperature was less than 40 °C.

## VII. REFERENCES

[1] IRENA, Solar PV in Africa: Costs and Markets, Chapter 3 Page 29

[2] Evans, D.L. 1981. Simplified method for predicting photovoltaic array output. Solar Energy 27, 555-560.

[3] Duffie, J.A., Beckman, W.A. 2006. Solar Energy Thermal Processes, third ed. Wiley, Hoboken, NJ, 23.3.

[4] A.Q. Jakhrani , "Comparison of Solar Photovoltaic Module Temperature Models", World Applied Sciences Journal 14 (Special Issue of Food and Environment): 01-08, 2011 ISSN 1818-495.

[4] E. Skoplaki, J.A. Palyvos. On the temperature dependence of photvoltaic module electrical performance: A review of efficiency/power correlations. Solar Energy 83 (2009) 614-624.

[5] Lasnier, F., Ang T.G., 1990. Photovoltaic Engineering Handbook. Adam Hilger, New York, NY, p.80.

[6] Koehl M, Heck M, Wiesmeier S, Wirth J. Modeling of the nominal operating cell temperature based on outdoor weathering. Sol Energ Mat Sol C 2011; 95: p. 1638-1646

[7] Kurtz S, Whitfield K, Miller D, Joyce J, Wohlgemuth J, Kempe M, et al. Evaluation of high-temperature exposure of rackmounted photovoltaic modules. In: 34th IEEE Photovoltaic Specialists Conference (PVSC), 2009: p. 2399-2404.

[8] E. Skoplaki, J.A. Palyvos. On the temperature dependence of photvoltaic module electrical performance: A review of efficiency/power correlations. Solar Energy 83 (2009) 614-624.

[9] A. Q. Malik, Lim Chee Ming, Tan Kha Sheng and M. Blundell; Influence of Temperature on the Performance of Photovoltaic

Corresponding Author Telephone: +821046309972
Email: hkahn@konkuk.ac.kr

[10] David L. King, Jay A. Kratochvil, and William E. Boyson Sandia National Laboratories, Albuquerque, NM; Temperature Coefficients For PV Modules and Arrays,1997.

[11] Dr. Won, L.Waithiru, D. Kim, B. Kang, K. Kim, G. Lee FLOATING PV POWER SYSTEM EVALUATION OVER FIVE YEARS (2011~2016 (EU PVSEC 2016)

[12] Martin A. Green, "High-Efficiency silicon solar cells", IEEE Transactions on electron Devices, Vol Ed-31 No.5, May 1984

[13] IEC Standard 61724, Photovoltaic system performance monitoring Guidelines for measurement, data exchange and analysis, 1993.

[14] A. Q. Malik, Lim Chee Ming, Tan Kha Sheng and M. Blundell; Influence of Temperature on the Performance of Photovoltaic, AJSTD Vol. 26 Issue 2 pp. 61-72 (2010)

[15] David L. King, Jay A. Kratochvil, and William E. Boyson Sandia National Laboratories, Albuquerque, NM; Temperature Coefficients For PV Modules and Arrays,1997.

[16] Ross, R.G., 1976. Interface design considerations for terrestrial solar cells modules, Proceedings of the 12th IEEE photovoltaic specialist's conference, Baton Rouge, LA, pp: 801-806.

[17] Rauschenbach, H.S., 1980. Solar cell array design handbook. Van Nosstrand Reinhold, New York, pp:390-391.

[18] Martin k.Fuentes Sandia National Laboratories;A Simplified Thermal Model for Flat-Plate Photovoltaic Arrays ( SAND85-0330•UC-63)

[19] Risser, V. V., and M. K. Fuentes. "Linear regression analysis of flat-plate photovoltaic system performance data." *5th Photovoltaic Solar Energy Conference*. 1984.

[20] Schott, T. "Operation temperatures of pv modules: a theoretical and experimental approach." *EC Photovoltaic solar energy conference. 6*. 1985.

[21] Servant, Jean-Micheal. "Calculation of the cell temperature for photovoltaic modules from climatic data." *Proceedings of the 9th biennial congress of ISES–Intersol*. Vol. 85. 1985.

[22] Corina MARTINEAC, Mihai HOPÎRTEAN, Gilbert DE MEY, Vasile ŢOPA, Silviu ŞTEFĂNESCU, "Temperature Influence on Conversion Efficiency in the Case of Photovoltaic Cells", 10th International Conference on DEVELOPMENT AND APPLICATION SYSTEMS, Suceava , Romania ,pp. 1-4, 2010

[23] IJIRSET, Latifa Sabri, Mohammed Benzirar, "Effect of Ambient Conditions on Thermal Properties of Photovoltaic Cells: Crystalline and AmorphousSilicon",DOI:10.15680/IJIRSET.2014.0312010

Corresponding Author Telephone: +821046309972

Email: hkahn@konkuk.ac.kr